

Fabrication of a New Porous Glass-Ceramic Monolith Using Vanadium(III) Calcium Phosphate Glass as Precursor

Italo Odone Mazali* and Oswaldo Luiz Alves

Instituto de Química, Universidade Estadual de Campinas, CP 6154, 13084-971 Campinas, SP - Brazil

Resultados preliminares de XRD, IR, Raman e SEM mostraram que monólitos vitrocerâmicos porosos (pgc-LVCP) com esqueleto tridimensional constituído pelas fases $V(PO_3)_3$ e $Ca_3(VO_4)_2$ foram obtidos utilizando um vidro original de $Li_2O-V_2O_5-CaO-P_2O_5$ como precursor. O pgc-LVCP pode ser um hospedeiro poroso promissor para sistemas químicos integrados visto que a fase $Ca_3(VO_4)_2$ apresenta propriedades ferroelétricas e de luminescência enquanto a fase $V(PO_3)_3$ exibe propriedades magnéticas associadas com elevada estabilidade mecânica, química e térmica.

Preliminary XRD, IR, Raman and SEM data indicate that porous glass-ceramic monoliths (pgc-LVCP) with skeleton of $V(PO_3)_3$ and $Ca_3(VO_4)_2$ with three-dimensional network structure using an original $Li_2O-V_2O_5-CaO-P_2O_5$ glass as precursor was obtained. The pgc-LVCP is a promising porous host for integrated chemical systems because the $Ca_3(VO_4)_2$ has ferroelectric and luminophor properties while $V(PO_3)_3$ exhibits magnetic properties associated with high degree of mechanical, chemical and thermal stability.

Keywords: porous materials, vanadium metaphosphate, calcium orthovanadate, vanadium glass, devitrification

Introduction

Porous materials are extremely important in the fields of nanotechnology, integrated chemical systems, and cooperative interactions in reactions performed in confined environment.¹⁻⁴ There is an increasing interest in designing and developing porous materials with stable porous texture for high-temperature separation and catalytic applications.⁵ It has been demonstrated that every property of nanophase materials is interesting for various technological applications because of the specifically size-related properties of crystalline domains or crystallites. In integrated chemical systems (ICS), the pore size of a support material determines the maximum size of the particle synthesized within it.^{2,6} The pores that typify these structures can be considered as 'micro-chambers', which fulfill, at the same time, a template role.^{7,8} The size, the morphology and the reactivity of the particle will depend on the dimensions, morphology, texture and chemical nature of the surface of pores.

As alternative to the silica skeleton, Kokubu and Yamane prepared a porous glass-ceramic with TiO_2 -rich skeleton by thermal treatment and posterior leaching of

the $TiO_2-SiO_2-Al_2O_3-B_2O_3-CaO-MgO$ glass.⁹ A spinoidal-type phase separation takes place during a two-step heat treatment of $6Li_2O-24TiO_2-39CaO-31P_2O_5$ glasses yielding $LiTi_2(PO_4)_3$, TiO_2 , $Li(TiO)PO_4$, $\beta-Ca_3(PO_4)_2$ and $\beta-Ca_2P_2O_7$ phases.^{10,11} Subsequent acid leaching removes the three last phases from the dense glass-ceramic and, as a result, a network of channels extends through the $LiTi_2(PO_4)_3$ with TiO_2 , as a minor phase. Recently, the preparation of a porous glass-ceramic with skeleton of $\alpha-NbPO_5$ with three-dimensional network structure from the glass system $Li_2O-Nb_2O_5-CaO-P_2O_5$ was reported.^{12,13} This was the first example, in the literature, of the preparation of a porous glass-ceramic where the devitrification occurs by surface crystallization, through heterogeneous nucleation.

The aim of this work was the fabrication and characterization of a porous glass-ceramic using an original vanadium(III) calcium phosphate glass as precursor. The phosphate framework exhibits great ability to stabilize reduced oxidation states because the relatively high charge in the PO_4^{3-} tetrahedral favors the formation of anionic frameworks with high degree of mechanical, chemical and thermal stability.¹⁴ Additionally, it is quite rare to find glassy porous materials other than siliceous materials.

* e-mail: mazali@iqm.unicamp.br

Experimental

Original glass samples of nominal composition $6\text{Li}_2\text{O}-18\text{V}_2\text{O}_3-43\text{CaO}-33\text{P}_2\text{O}_5$ (mol %), g-LVCP, were prepared by melting reagent grade Li_2CO_3 , CaCO_3 , V_2O_5 and P_2O_5 in a platinum crucible at $1450\text{ }^\circ\text{C}$ for 1 h under air. The melt was poured onto carbon plates and annealed at $490\text{ }^\circ\text{C}$ for 2 h (the glass transition temperature, T_g , is equal to $530\text{ }^\circ\text{C}$). Glass-ceramic samples (gc-LVCP) were prepared by a thermal treatment of the glass plates at $530\text{ }^\circ\text{C}$ for 20 h (nucleation step) and subsequently at $600\text{ }^\circ\text{C}$ for 12 h (crystallization step; the crystallization temperature, T_c , is equal to $600\text{ }^\circ\text{C}$ for g-LVCP for a heating rate of $10\text{ }^\circ\text{C min}^{-1}$). The resulting glass-ceramics (gc-LVCP) was immersed in 1.0 mol L^{-1} HCl aqueous solution and kept for 24 h at room temperature, in order to obtain porous glass-ceramic (pgc-LVCP).

Powder X-ray diffraction (XRD) patterns were obtained using a Shimadzu XRD6000 diffractometer, with Ni filters and $\text{CuK}\alpha$ radiation, using 30 kV and 20 mA, calibrated with Si at a $2^\circ/\text{min}$ rate. Infrared spectra (IR) of KBr pellets were measured with a Perkin Elmer 1600 FTIR in the $1400-400\text{ cm}^{-1}$ range, with a resolution of 2 cm^{-1} . The Raman spectra were recorded on a Renishaw System 3000 Raman Imaging Microscope (*ca.* $1\text{ }\mu\text{m}$ spatial resolution) using a He-Ne laser (632.8 nm) and 8 mW of power before the entrance optics. Scanning electron microscope (SEM) was performed by using a JEOL JSM T-300 Microscope. The density of pg-LVCP and pgc-LVCP were measured by the Archimedes's method using deionized water as the buoyancy liquid at $25\text{ }^\circ\text{C}$.

Results and Discussion

The crystalline phases of the glass-ceramic before and after acid leaching were characterized by X-ray powder diffraction (XRD), infrared (IR) and Raman spectroscopies. In spite of the very close interplanar distances, the XRD pattern (Figure 1) suggested the presence of the following phases in dark green gc-LVCP: $\beta\text{-Ca}_2\text{P}_2\text{O}_7$ ¹⁵, $\beta\text{-Ca}_2\text{V}_2\text{O}_7$ ¹⁶, $\beta\text{-Ca}_3(\text{PO}_4)_2$ ¹⁵, $\text{Ca}_3(\text{VO}_4)_2$ ¹⁵, $\text{V}(\text{PO}_3)_3$ ¹⁵, VPO_4 ¹⁵ and LiCaPO_4 ¹⁵ phases. The dark green color of the gc-LVCP is due to the occurrence of the $\text{V}(\text{PO}_3)_3$ and $\beta\text{-Ca}_2\text{V}_2\text{O}_7$ phases. The phases identified show mixed valence state vanadium, but the presence of $\text{V}(\text{PO}_3)_3$ and VPO_4 phases confirms the stabilization of vanadium as V(III). In the XRD pattern of the pgc-LVCP, the absence of peaks at 27.0° , 28.5° and 33.5° (2θ) confirms the leaching of the $\beta\text{-Ca}_2\text{P}_2\text{O}_7$, $\beta\text{-Ca}_2\text{V}_2\text{O}_7$ and LiCaPO_4 phases, respectively. The leaching of the VPO_4 phase is confirmed by the absence of peaks at 24.8° and 35.4° (2θ) in pgc-LVCP.

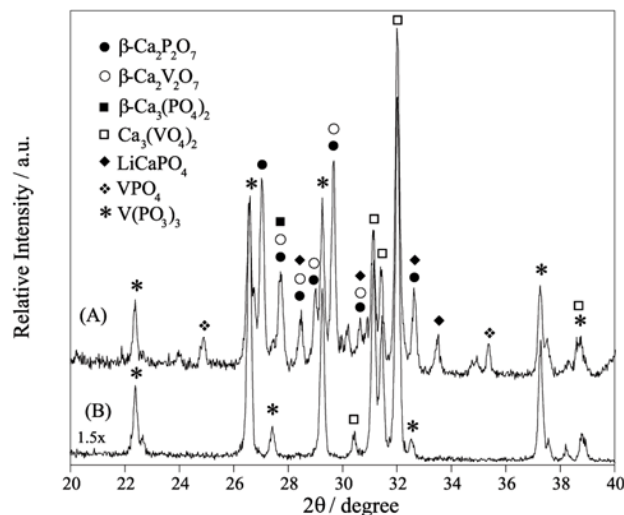


Figure 1. Powder XRD patterns of (A) gc-LVCP and (B) pgc-LVCP.

The IR spectrum of gc-LVCP sample (Figure 2) confirmed the presence of pyrophosphate groups, characterized by the following typical modes: $\nu(\text{PO}_3)_{\text{asym}}$ (between 1210 cm^{-1} and 1100 cm^{-1}), $\nu(\text{PO}_3)_{\text{sym}}$ (between 1065 cm^{-1} and 1000 cm^{-1}), $\nu(\text{P-O-P})_{\text{asym}}$ (972 cm^{-1} and 944 cm^{-1}) and especially by the band at 725 cm^{-1} , characteristic of the $\beta\text{-Ca}_2\text{P}_2\text{O}_7$, $\nu(\text{P-O-P})_{\text{sym}}$ mode.¹⁷ The occurrence of this group is also confirmed by Raman spectroscopy (Figure 3), with a band at 737 cm^{-1} [$\nu(\text{PO}_3)_{\text{sym}}$]. The occurrence of the $\beta\text{-Ca}_2\text{V}_2\text{O}_7$ phase is confirmed by the presence of bands of $\text{V}_2\text{O}_7^{4+}$ groups: at 874 cm^{-1} (IR) and 880 cm^{-1} (Raman) attributed to $\nu_{q4}(\text{V-O})$ and by IR bands at 815 cm^{-1} [$\nu_{q6, q7}(\text{V-O})$], 530 cm^{-1} and 472 cm^{-1} [$\nu(\text{V-O-V})_{\text{sym}}$].¹⁸ In the gc-LVCP, there is overlapping of the $\text{Ca}_3(\text{VO}_4)_2$ and $\beta\text{-Ca}_3(\text{PO}_4)_2$ bands in IR spectra, but the Raman spectra permit distinguishing between these isostructural phases. The Raman bands in $\text{Ca}_3(\text{VO}_4)_2$ are distributed in only two wavenumber regions relating to the $\nu(\text{V-O})$ modes ($950-750\text{ cm}^{-1}$; observed at 900 cm^{-1} as a very strong band in both gc-LVCP and pgc-LVCP) and $\delta(\text{O-V-O})$ modes mixed with the translational and rotational modes of the VO_4^{3-} groups as well as Ca^{2+} cations displacements ($50-450\text{ cm}^{-1}$).¹⁹ The Raman bands in $\beta\text{-Ca}_3(\text{PO}_4)_2$ are distributed in five distinct wavenumber ranges: $170-305$, $405-483$, $547-631$, $946-970$, and $1005-1091\text{ cm}^{-1}$, corresponding to the lattice modes and, ν_2 , ν_4 , ν_1 and ν_3 internal modes of the PO_4^{3-} ions, respectively.¹⁹ The IR and Raman spectra of the pgc-LVCP are simpler, in comparison to these of gc-LVCP. The acid leaching of the $\beta\text{-Ca}_2\text{P}_2\text{O}_7$ and $\beta\text{-Ca}_2\text{V}_2\text{O}_7$ phases were confirmed by the absence of bands at 725 cm^{-1} (IR) and 737 cm^{-1} (Raman); and at 880 cm^{-1} (Raman), respectively. The occurrence of the $\beta\text{-Ca}_3(\text{PO}_4)_2$ phase is confirmed by presence and subsequent absence of Raman bands at 572 , 600 and 652 cm^{-1} before and after leaching, respectively. pgc-LVCP

exhibits a bright green color due the presence of $V(PO_3)_3$, confirmed by the peaks at 22.5° , 26.5° , 29.2° and 37.2° (2θ) in the XRD pattern (Figure 1). The $V(PO_3)_3$ phase can be described as being formed from isolated VO_6 octahedra linked through infinite $[PO_3]_n$ chains of PO_4 tetrahedra. Each VO_6 group is bridged to six neighbouring VO_6 by phosphate groups. These lie in one of the two adjacent layers and lead to three dimensional bonding. The V^{3+} -O bond length, in VO_6 geometry, is moderately distorted.¹⁴ Higher valence vanadium systems are characterized by the short vanadyl bond ($V=O$) responsible for a highly intense Raman band at 994 cm^{-1} .²⁰ The absence of this band in both gc-LVCP and pgc-LVCP confirmed the occurrence of $V(PO_3)_3$.

Scanning electron microscopy (SEM) of the fracture face confirmed the porous structure of the pgc-LVCP, which exhibits a popsicle-like structure (Figure 4), as a

consequence of devitrification that occurs by surface crystallization and the process proceeds from the surface to the bulk of the specimen.

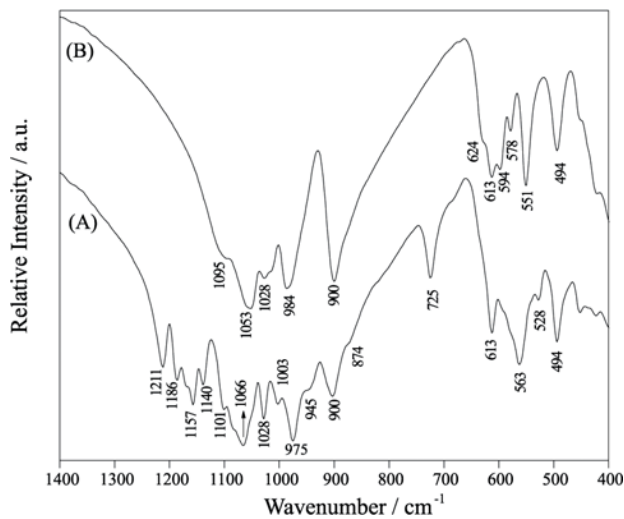


Figure 2. Infrared spectra of (A) gc-LVCP and (B) pgc-LVCP.

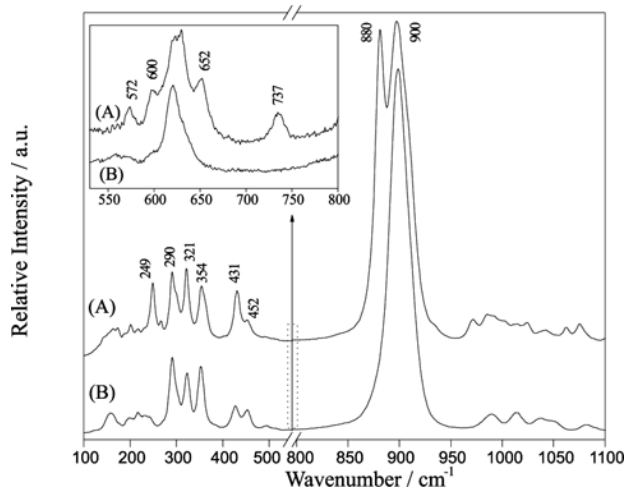


Figure 3. Raman spectra of (A) gc-LVCP and (B) pgc-LVCP.

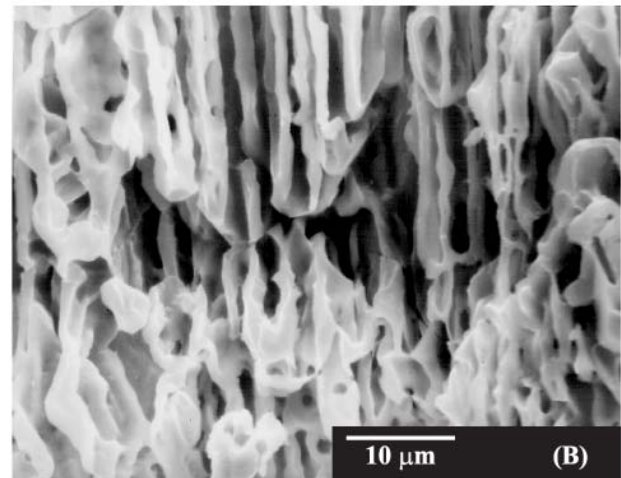
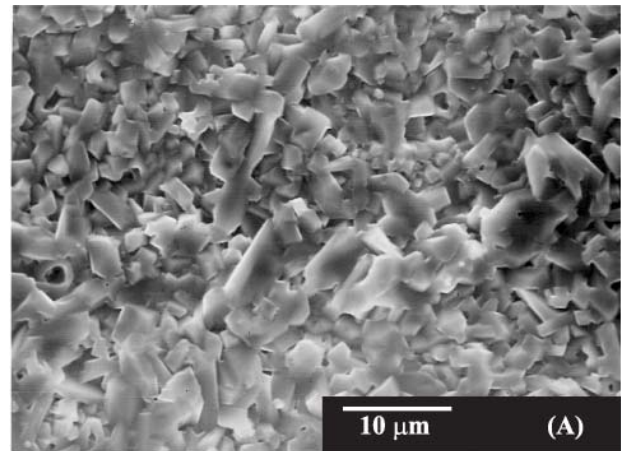


Figure 4. SEM micrographs of the fracture face of (a) gc-LVCP and (b) pgc-LVCP.

The bulk densities of the pg-LVCP and pgc-LVCP, measured by Archimedes's method, are 3.10 g cm^{-3} and 1.76 g cm^{-3} , respectively. The apparent density of the ceramic skeleton of the pgc-LVCP is 3.14 g cm^{-3} [for comparison, for the $V(PO_3)_3$ phase it is 3.03 g cm^{-3} and for the $Ca_3(VO_4)_2$ phase it is between 3.17 - 3.50 g cm^{-3} depending on the polymorph]. In the apparent density it is just considered the occupied volume by the ceramic skeleton in the monolith. The leachability is the measure of the occupied volume for the soluble phases that constitute the gc-LVCP. Therefore, the leachability correspond the porosity presented by the pgc-LVCP. The leachability is calculated using the equation:

$$\text{Leachability} = \left(1 - \frac{\rho_{\text{bulk}}}{\rho_{\text{apparent}}} \right) \cdot 100 \quad (1)$$

where, ρ_{bulk} is the bulk density and ρ_{apparent} is the apparent density of the pgc-LVCP. Therefore, the gc-LVCP exhibits leachability up to approximately 45 vol.%.

In summary, the preliminary data reported here allows us to conclude that fabrication of porous glass-ceramic monoliths with skeleton of $V(\text{PO}_3)_3$ and $\text{Ca}_3(\text{VO}_4)_2$ and having a three-dimensional network structure using vanadium phosphate glass as precursor, was obtained and is reported here for the first time. The pgc-LVCP can be a promising porous host for ICS because $\text{Ca}_3(\text{VO}_4)_2$ phase has ferroelectric and luminophor properties^{19,21} while the $V(\text{PO}_3)_3$ phase exhibits magnetic property associated with high degree of mechanical, chemical and thermal stability.¹⁴ Further studies are being carried out in our laboratory aimed at the stoichiometric determination of the phases as well as the control of composition phases and the use of these porous materials as host for integrated chemical systems.

Acknowledgment

The authors are grateful to Prof. D.L.A. Faria and Prof. M.L.A. Temperini (IQ-USP, Brazil) for the Raman measurements and to Prof. C.H. Collins (IQ-UNICAMP, Brazil) for English revision. This is a contribution of the Millennium Institute for Complex Materials (PADCT/MCT).

Reference

1. Cassagneau, T.; Hix, G.B.; Jones, D.J.; Maireles-Torres, P.; Rhomani, M.; Rozière, J.; *J. Mater. Chem.* **1994**, *4*, 189.
2. Bard, A.J.; *Integrated Chemical Systems – An Approach to Nanotechnology*, Wiley : New York, 1994.
3. Gimenez, I.F.; Alves, O.L.; *J. Braz. Chem. Soc.* **1999**, *10*, 167.
4. Maia, D.J.; Zarbin, A.J.G.; Neves, S.; De Paoli, M.A.; Alves, O.L.; *Quim. Nova* **2000**, *23*, 204.
5. Kumar, K.N.P.; *Appl. Catal. A* **1994**, *119*, 163; Kumar, K.N.P.; Keizer, K.; Burggraaf, A.J.; *J. Mater. Sci. Lett.* **1994**, *13*, 59.
6. Mazali, I.O.; Alves, O.L.; *J. Phys. Chem. Solids*, submitted.
7. Schmelzer, J.; Möller, J.; Slezov, V.V.; *J. Phys. Chem. Solids*, **1995**, *56*, 1013.
8. Mazali, I.O.; *Ph.D. Thesis*, Universidade Estadual de Campinas, Brazil, 2001.
9. Kokubu, T.; Yamane, M.; *J. Mater. Sci.* **1985**, *20*, 4309.
10. Hosono, H.; Abe, Y.; *J. Non. Cryst. Solids* **1995**, *190*, 185.
11. Gimenez, I.F.; Mazali, I.O.; Alves, O.L.; *J. Phys. Chem. Solids* **2001**, *62*, 1251.
12. Mazali, I.O.; Alves, O.L.; *J. Mater. Sci. Lett.* **2001**, *20*, 2113.
13. Mazali, I.O.; Barbosa, L.C.; Alves, O.L.; *J. Mater. Sci.* **2004**, *39*, 1987.
14. Rojo, J.M.; Mesa, J.L.; Calvo, R.; Lezama, L.; Olazcuaga, R.; Rojo, T.; *J. Mater. Chem.* **1998**, *8*, 1423; Middlemiss, N.; Hawthorne, F.; Calvo, C.; *Can. J. Chem.* **1977**, *55*, 1673.
15. Joint Committee on Powder Diffractions Standards. For $\beta\text{-Ca}_2\text{P}_2\text{O}_7$ card 20-24; $\beta\text{-Ca}_3(\text{PO}_4)_2$ card 32-176; $\text{Ca}_3(\text{VO}_4)_2$ card 46-756; $V(\text{PO}_3)_3$ card 33-1442; VPO_4 card 34-1336; LiCaPO_4 card 14-403.
16. Krasnenko, T.I.; Andrianova, L.V.; Zolotukhina, L.V.; Fotiev, A. A.; *Inorg. Mater.* **1998**, *34*, 733; Nord, A.G.; Åberg, G.; Stefanidis, T.; Kierkegaard, P.; Grigoriadis, V.; *Chem. Scr.* **1985**, *25*, 212.
17. Waal, D.; Hutter, C.; *Mater. Res. Bull.* **1994**, *29*, 1129.
18. Kristallov, L.V.; Fotiev, A.A.; Tsvetkova, M.P.; *Russ. J. Inorg. Chem.* **1982**, *27*, 1714.
19. Grzechnik, A.; *Chem. Mater.* **1998**, *10*, 1034; Leonidov, I.A.; Leonidova, O.N.; Surat, L.L.; Kristallov, L.V.; Perelyaeva, L.A.; Samigullina, R.F.; *Russ. J. Inorg. Chem.* **2001**, *46*, 268.
20. Stranford, G.T.; Condrate, R.A.; *J. Solid State Chem.* **1984**, *52*, 248.
21. Grzechnik, A.; *Solid State Sci.* **2002**, *4*, 523.

Received: April 30, 2004

Published on the web: August 10, 2004

FAPESP helped in meeting the publication costs of this article.